

# Molecular structure and chemical bonding in $K_3C_{60}$ and $K_6C_{60}$

Wanda Andreoni

*IBM Research Division, Zurich Research Laboratory, CH-8803 Rüschlikon, Switzerland*

Paolo Giannozzi

*Istituto Nazionale Fisica della Materia, Forum for Theoretical Physics,  
Scuola Normale Superiore, piazza dei Cavalieri 7, I-56126 Pisa, Italy  
and IBM Research Division, Zurich Research Laboratory, CH-8803 Rüschlikon, Switzerland*

Michele Parrinello\*

*IBM Research Division, Zurich Research Laboratory, CH-8803 Rüschlikon, Switzerland*

(Received 5 August 1994)

We present the results of local-density-approximation-based Car-Parrinello calculations of orientationally ordered phases of  $K_3C_{60}$  and  $K_6C_{60}$ . Our investigation focuses on the following points: the effects of alkali-metal intercalation on the structural and electronic properties of  $C_{60}$ , the chemical bonding, the inhomogeneity of the electron distribution, and the degree of freedom of the potassium atoms in the interstitial region. The results are discussed in view of experimental data, such as x-ray and neutron-diffraction data as well as nuclear magnetic resonance spectroscopy.

## I. INTRODUCTION

K and Rb intercalated  $C_{60}$  are the fullerene-based materials that have been most extensively studied in the past few years.<sup>1-3</sup> Depending on the alkali-metal concentration, both structural and electronic properties change in a drastic and nontrivial manner. The main drive in this research has come from the discovery that the  $x = 3$  phases were superconductors at relatively high temperatures.<sup>4-6</sup> The  $x = 6$  compounds were readily obtained and were soon found to be the saturated phases. They provide stable new insulating materials,<sup>7</sup> which are often used as the primary compounds to synthesize fullerides of lower alkali-metal concentration. Although all possible and sophisticated experimental methods have been used for the investigation of the structural and electronic properties of these materials, several questions remain open concerning basic physical properties,<sup>8,9</sup> such as the state of orientational disorder in the  $x = 3$  phases<sup>10</sup> and its consequences for superconductivity,<sup>11</sup> the different behavior of the K and Rb compounds emerging especially from electron spin resonance spectroscopy,<sup>8</sup> the nonmetallic nature of the  $x = 4$  phases,<sup>12,13</sup> and even the sample and stoichiometry dependence of some physical characteristics.<sup>14</sup> Theoretical work has focused on one hand on the search for a plausible mechanism of the superconductivity of the  $x = 3$  phases<sup>15-17</sup> and on the other hand on the calculation of the electronic energy bands.<sup>12,18-20</sup> While a very simple approach such as a rigid band scheme built from the Hückel molecular energy levels provides a preliminary understanding of the electronic structure of the fullerides, it is soon seen that also more sophisticated calculated energy bands are not sufficient to explain a number of experimental data, such as photoemission spectra (PES).<sup>21,22</sup> Model calculations have also been performed to study the effect of orientational disorder<sup>11,12,23-25</sup> on the band structure of the  $x = 3$  solids and to unravel the effects of electron-phonon

and electron-plasmon couplings.<sup>26</sup> Here, we concentrate on a different aspect of the chemico-physical properties of the  $K_xC_{60}$  compounds, which has been widely neglected so far: the effects of K doping on the molecular structure and its influence on the electronic properties. The density functional theory in the local density approximation (LDA) for the exchange and correlation functional is the scheme adopted for the electronic problem. The basic tool we use to optimize the molecular structure is the Car-Parrinello method,<sup>27</sup> whereas the lattice parameter is taken from experiment. This approach allows us to discuss in some detail the character of the chemical bonding. In particular, our analysis (i) will determine the amount of charge transfer from the alkali-metal atoms to the fullerene, (ii) will isolate its influence from that of solid-state effects on the molecular architecture, and in turn (iii) will establish to what extent K intercalation can be considered as a perturbation on the electronic structure of the "host" molecular solid. Also, our calculations allow us to establish some (hitherto neglected) features of the electron density distribution, such as its inhomogeneity at the molecular level as well as in the interstitial region, which should be of help for the interpretation of nuclear magnetic resonance (NMR) spectroscopy data.<sup>8</sup> Our study can be considered rather complete for the case of  $K_6C_{60}$ . In contrast, as concerns  $K_3C_{60}$ , the study of the link between geometrical and electronic structures requires further work aimed at including at least the effects of orientational disorder.

## II. COMPUTATIONAL SCHEME

The input of the calculations consists of the crystal structure, which is taken from experiment,<sup>7,28</sup> and of the atomic pseudopotentials. For the crystal structure, in line with previous *ab initio* LDA calculations made so far, we consider the molecules to be orientationally or-

TABLE I. Parameters of the relativistic local ( $s$ ) pseudopotential used for K (in a.u.). The analytical expression is  $V_0(r) = -\text{erf}(r/r_c)/r + (a_0 + b_0r^2)\exp[-(r/r_0)^2]$ . The core charge is given by  $(\alpha + \beta r^2)\exp[-(r/R_{cc})^2]$  (see Ref. 31).

$r_c$	$r_0$	$a_0$	$b_0$	$\alpha$	$\beta$	$R_{cc}$
1.889822	1.28037	2.585104	0.534834	0.013195	0.005344	1.668

dered in both  $\text{K}_3\text{C}_{60}$  and  $\text{K}_6\text{C}_{60}$ . Consistently with the scheme adopted here for the solids, the pseudopotentials are derived from LDA all-electron calculations and are norm conserving. The carbon pseudopotential is given in Ref. 29, and the one for potassium is given in Table I. Potassium is considered as a one-valence-electron system. An accurate treatment of alkali metals as one-electron systems requires the explicit inclusion of non-linear core corrections in the exchange-correlation LDA functional.<sup>30-32</sup> We expand the electron wave functions in plane waves up to an energy cutoff of 35 Ry.<sup>33</sup> The calculations are performed in two steps. First, by using electron-ion combined steepest descent and molecular dynamics (Car-Parrinello) procedures, we relax the atomic positions in a periodically repeated unit cell containing only one  $\text{C}_{60}$ . This is equivalent to a self-consistent calculation using only  $k = 0$  as representative of the Brillouin zone for the electron density. Second, starting with the structure thus obtained, we perform a more traditional LDA calculation of the forces using two Chadi-Cohen<sup>34</sup>  $k$  points for the fcc and the  $P$  point for the bcc structures. At the final geometry for the molecule, the forces on the carbon atoms had an average deviation from zero of  $10^{-4}$  a.u. The deviation of the structural parameters thus obtained from those calculated with  $\Gamma$  only in the irreducible Brillouin zone was sizable (as will be shown in Sec. III). In contrast, the energy bands calculated at fixed geometry converge much more rapidly, and no significant difference could be seen. Using  $\text{K}_3\text{C}_{60}$  as the test system, we have checked the convergence of the forces in terms of the irreducible Brillouin zone mesh by performing a calculation with ten Chadi-Cohen<sup>34</sup>  $k$  points. We found that, at the equilibrium geometry obtained with the two Chadi-Cohen points, the forces changed by less than  $10^{-5}$  a.u., i.e., less than the accuracy itself of the calculations.

### III. RESULTS

#### A. Molecular structure

The crystal structure of  $\text{K}_3\text{C}_{60}$  and  $\text{K}_6\text{C}_{60}$  has been established through x-ray diffraction (XRD) at room temperature.<sup>7,28,35</sup>  $\text{K}_6\text{C}_{60}$  is bcc with space group  $Im\bar{3}$  and a lattice constant of  $a = 11.38$  Å. The molecules are orientationally ordered<sup>36</sup> (with orientation  $T_h^3$ ) [see Fig. 1(a)]. In  $\text{K}_3\text{C}_{60}$ , the  $\text{C}_{60}$  centers occupy the sites of a fcc lattice with a spacing of  $a = 14.24$  Å. The refinement of XRD data<sup>35</sup> suggests a picture in which the molecules randomly assume two inequivalent relative orientations related by a  $\pi/2$  rotation about a twofold axis ("merohedral" disorder). The orientationally or-

dered configuration we assume here, in line with previous LDA band structure calculations, corresponds to the  $T_h^3$  orientation<sup>36</sup> (space group  $Fm\bar{3}$ ) [see Fig. 1(b)]. As is especially apparent from NMR relaxation experiments,<sup>37</sup> in bcc  $\text{K}_6\text{C}_{60}$  the  $\text{C}_{60}$  molecules are ordered at all temperatures, while this is not the case for  $\text{K}_3\text{C}_{60}$  where some kind of orientational disorder persists down to low temperatures.<sup>38,39</sup> Also in this case, however, our ordered structural model should not be restrictive for our study

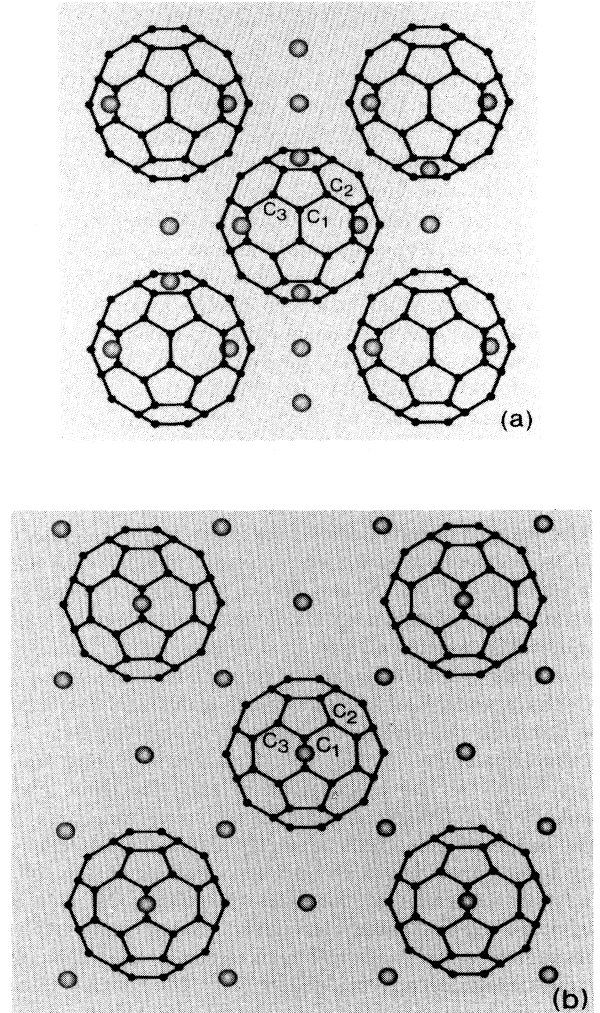


FIG. 1. Structure of the ordered configurations considered in the present work. (a) bcc  $\text{K}_6\text{C}_{60}$  (111) plane, and (b) fcc  $\text{K}_3\text{C}_{60}$  (100) plane.  $C_1$ ,  $C_2$ , and  $C_3$  denote the three inequivalent atoms.

of primary interest here, namely, for the characterization of the major “on-ball” effects of the interaction between the alkali metals and the fullerenes.

The modification of the structure of the  $C_{60}$  molecule in the alkali-metal fullerenes can be considered the result of three different processes: the confinement in a finite box, the lowering of symmetry due to the crystal field, and the electron donation from the dopants. The former two contributions are also present in the  $C_{60}$  fullerite. However, being that the interaction between the molecules is weak, one can expect their effects to be negligible at the density of the alkali-metal fullerenes. From organic chemistry<sup>40</sup> and observations on graphite alkali-metal intercalated compounds,<sup>41</sup> it is known in contrast that electron donation can modify carbon-carbon bonds significantly and in a selective manner. Here, we shall obtain all these effects through a set of calculations: on the isolated molecule ( $C_{60,m}$ ),<sup>42</sup> on the fcc and bcc  $C_{60}$  fullerites at the density of  $K_3C_{60}$  (fcc  $C_{60,m}$ ), and  $K_6C_{60}$  (bcc  $C_{60,m}$ ), respectively, and on the two fullerenes with fully relaxed atomic positions, as well as with the molecular structure kept fixed<sup>43</sup> ( $K_xC_{60,m}$ ). Finally, calculations on the fcc and bcc  $C_{60}$  fullerites ( $C_{60,d}$ ), with the molecular structure deformed as in the optimized fullerenes, will help us understand the process of electron donation.

The cubic crystal field splits the carbon sites into three nonequivalent sets:  $C_1, C_2, C_3$ , as shown in Fig. 1, in the ratio 1:2:2. This gives rise to five different bond lengths. The calculated values are reported in Table II and compared with those obtained for the isolated molecule<sup>42</sup> and for the fcc and bcc  $C_{60}$  fullerites at the densities of  $K_3C_{60}$  and  $K_6C_{60}$ , respectively. The comparison shows that, as expected, the dominant effect by and large is that of the electron transfer from the alkali-metal atoms to the molecule, and that this is bond selective. As a result, the  $C_{60}$  molecule deforms mainly due to the reduction of the bond alternation through the weakening of the double bonds, and only to a minor extent are the crystal field splittings emphasized in the presence of the K atoms. Clearly, such effects increase with increasing alkali-metal concentration. The weakening of the double bonds resulting from electron donation can be understood simply

in terms of a decrease in the  $\pi$ -bond order,<sup>40</sup> because the excess electrons occupy the lowest unoccupied ( $t_{1u}$ ) orbitals of  $C_{60}$ , which are antibonding on the double bonds. The antibonding character is clearly seen in Fig. 2, where we plot the density of the occupied  $t_{1u}$ -derived states in  $K_3C_{60}$  on the plane of a hexagon. The  $C_1$ - $C_1$  and  $C_2$ - $C_3$  lines correspond to double bonds. On the single bonds ( $C_1$ - $C_2$  line), instead, the  $t_{1u}$ -derived states are weakly bonding, hence the weak effect of electron donation, and, if any, a small shrinking of these bond lengths.<sup>44</sup> The bond alternation is preserved in both compounds, but the difference of the bond lengths decreases from 0.06 Å in the undoped systems to average values of 0.04 Å in  $K_3C_{60}$  and 0.02 Å in  $K_6C_{60}$ . These results are in agreement with recent neutron-diffraction data on both  $K_3C_{60}$  and  $K_6C_{60}$ .<sup>45</sup> Neutron diffraction data on  $Na_2CsC_{60}$ , on the other hand, seem to suggest that the bond alternation is already lost under donation of three electrons to  $C_{60}$ .<sup>46</sup> However, we note that  $Na_2CsC_{60}$  has a different structure, namely, a simple cubic one with four molecules per unit cell, and that the orientational disorder in all the  $x = 3$  compounds may render the experimental determination of the molecular features difficult.

As reported in Table II, the average carbon-carbon distance is rather constant; so is the average  $C_{60}$  radius, which changes from 3.53 Å in the molecule to 3.55 Å in  $K_3C_{60}$  and 3.56 Å in  $K_6C_{60}$ . The difference in radii of the three inequivalent carbon atoms, however small, can be observed experimentally.<sup>45</sup> In agreement with these experiments, our calculations show that in  $K_6C_{60}$  the  $C_3$  atom [see Fig. 1(b)] is pushed inward by  $\approx 0.01$  Å with respect to  $C_1$  and  $C_2$ . In  $K_3C_{60}$ , the noticeable difference is on  $C_1$  [see Fig. 1(a)], which is pushed outward by  $\approx 0.02$  Å with respect to the other two. Only minor distortions of the bond angles result from our calculations. The root mean square deviations from 120° and 108° do not exceed 0.2° in both cases, with maximum deviations of 0.3°.

The energy gain associated with the relaxation of the molecular structure in the fullerenes amounts to only a few tenths of an eV, i.e., 0.18 eV in  $K_3C_{60}$  and 0.54 eV in  $K_6C_{60}$ . Such molecular deformations would instead be unfavored in the undoped materials and cost similar

TABLE II.  $K_3C_{60}$  and  $K_6C_{60}$ : interatomic distances in Å. The three nonequivalent C atoms are denoted as in Fig. 1. For comparison, the calculated values in the isolated molecule and in fcc and bcc  $C_{60}$  are also listed. The K-C distances are the closest ones. See text.

$i$	$j$	$K_3C_{60}$	$K_6C_{60}$	fcc $C_{60}$	bcc $C_{60}$	$C_{60}$
$C_1$	$C_1$	1.410	1.428	1.391	1.390	1.390
$C_2$	$C_3$	1.406	1.420	1.393	1.393	1.390
$C_1$	$C_2$	1.446	1.445	1.448	1.448	1.447
$C_2$	$C_3$	1.446	1.442	1.449	1.445	1.447
$C_3$	$C_3$	1.443	1.440	1.451	1.450	1.447
$\bar{C}$	$\bar{C}$	1.433	1.435	1.430	1.429	1.428
$K_T$	$C_{2,3}$	3.252				
$K_O$	$C_1$	3.697				
K	$C_1$		3.282,3.448			
K	$C_2$		3.319,3.367			
K	$C_3$		3.191,3.500			

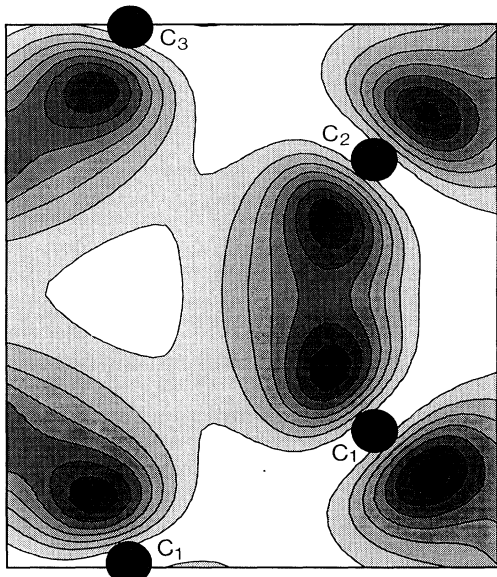


FIG. 2.  $K_3C_{60}$ : density distribution of the  $t_{1u}$ -derived electron states on the plane of a hexagon. Contours scale linearly from 0.0002 to 0.0014  $e/(a.u.)^3$ .

energy amounts: 0.14 eV and 0.48 eV, respectively.

Some of us<sup>47</sup> have previously calculated these effects in the case of the  $Li_{12}C_{60}$  molecule, which retains the icosahedral symmetry. Here twelve electrons are essentially transferred to the  $C_{60}$  ball and occupy the  $t_{1g}$  orbitals as well, which are similar in character to the  $t_{1u}$ 's. As a consequence, the shortest carbon-carbon distances at the hexagon-hexagon junctions increase so much as to render the bond alternation negligible (0.01 Å).

Concerning the location of the K atoms, we have verified with molecular dynamics runs that in  $K_3C_{60}$  the configuration with two K's in the crystallographic (*c*) *T* sites and one in the (*b*) *O* position corresponds to a well-defined minimum of the potential energy surface. The  $K_O$ , however, having a larger void around it, can move more easily than the  $K_T$ 's. This was apparent in our molecular dynamics simulations. Figure 3(a) shows the result of calculations performed on geometries with the potassium atom away from the *O* site  $(1/2, 0, 0)a$  on the (100) direction  $(1/2 - \delta, 0, 0)a$  (the molecular structure is relaxed for each K position). The effect on the energy is still negligible for displacements as large as  $\approx 0.8$  Å. This result is consistent with the fact that the thermal factor given by structural refinement<sup>35</sup> is larger for  $K_O$  than for  $K_T$  by more than 50%. Very recent XRD data<sup>48</sup> show that even at low temperatures the Debye-Waller factor of  $K_O$  is anomalously high. This has been interpreted as a sign of positional (static) disorder.

In  $K_6C_{60}$ , the K's occupy the (*e*)  $(1/4 - \delta, 1/2, 0)a$  positions on the faces of the cube. Our optimized value for the deviation from the tetrahedral sites ( $\delta = 0$ ) is  $\delta = 0.026$ , which compares well with the XRD refined value for  $Cs_6C_{60}$ :  $\delta = 0.028$ . In addition, this distortion was slightly exaggerated in the calculations using only the  $\Gamma$  point to represent the irreducible Brillouin zone.<sup>49</sup>

The behavior of the energy as a function of  $\delta$  is shown in Fig. 3(b). It is extremely flat for variations of  $\delta$  of  $\approx 0.01$  around the optimal value. Electrostatic forces are the main factor determining the distortion from the tetrahedral positions as well as the anisotropy around  $\delta = 0$ .

## B. Chemical bonding and other electronic properties

By examining the spatial distribution of the valence electron density and of the individual Kohn-Sham orbitals, we obtain an overall picture of the chemical bonding and of the effects of the potassium intercalation on the electronic properties of the molecule. In order to investigate further the inhomogeneity of the electron distribution in a semiquantitative manner, we divide the space into Voronoy polyhedra<sup>50</sup> [i.e., Wigner-Seitz-like (WS) cells] and perform the integrations there, thus attributing each mesh point to the closest atom. We have checked that all valence states have purely molecular character. Therefore, integrals in the region of the K's provide a

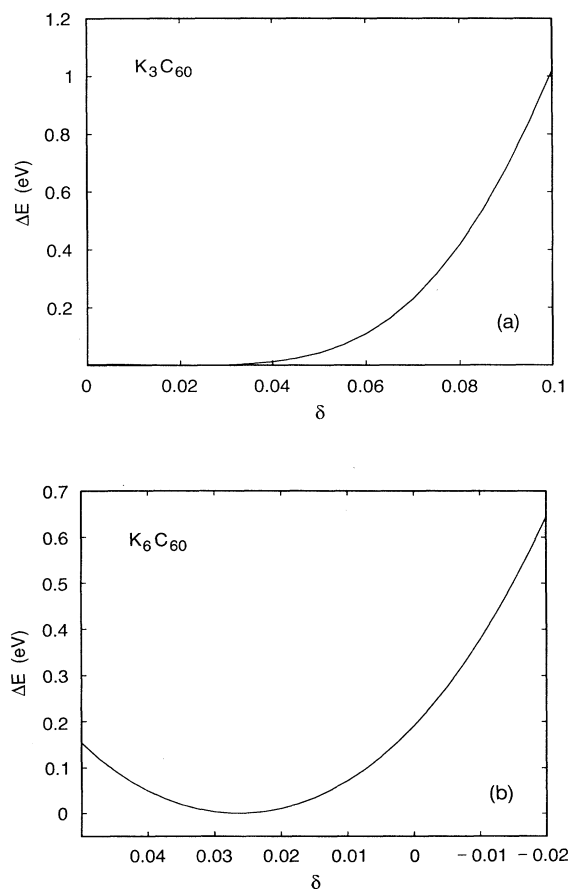


FIG. 3. Energy change (in eV) as a function of the displacement of the K atoms. (a)  $K_3C_{60}$ : the displacement refers to the K atom on the *O* site  $(0.5, 0, 0)a$  ( $\delta = 0$ ) and is made along the (100) direction; (b)  $K_6C_{60}$ :  $\delta$  is measured with respect to the tetrahedral sites on the faces of the cube;  $\delta = 0.026$  corresponds to the equilibrium positions.

measure of the extension of the molecular orbitals in the interstitial regions, rather than of the mixture with K atomic orbitals.

In Figs. 4 and 5, we plot (a) the total valence electron density  $\rho(r)$ , (b) the density  $\rho_{t_{1u}}$  of the occupied  $t_{1u}$ -derived states, (c) the excess electron density  $\Delta_d(r) = \rho(r) - \rho_{C_{60},d}(r)$ , and (d) the transfer density  $\Delta_t(r) = \rho(r) - \rho_{C_{60},d}(r) - \rho_{K_x}(r)$ , where  $\rho_{K_x}(r)$  is the superposition of the atomic charges. The plots are on the (110) plane of the fcc cell for  $K_3C_{60}$  and on the (100) plane of the bcc cell for  $K_6C_{60}$ . The same comments apply to both cases. Although strongly localized on the  $C_{60}$  molecules,  $\rho(r)$  extends appreciably in the interstitial region, as previously noted in Ref. 19. If the molecules were passive charge acceptors, the excess electron density  $\Delta_d(r)$  would coincide with that of the  $t_{1u}$ -derived states. This is not the case, as seen by comparing Fig. 4(b) with Fig. 4(c), and Fig. 5(b) with Fig. 5(c). In fact, as we have noted previously,<sup>47,49,51</sup> the distribution of the excess electrons on alkali-metal fullerenides is much more

complex and reflects the strong polarization of the  $C_{60}$  electronic structure in response to the presence of electron donors. This fact also emerges from Fig. 6, where we plot around the molecular center the spherical average of the density of the  $t_{1u}$ -derived states, of the excess electron density, and their difference as well as their integrals as a function of the distance  $R$  from the center [ $I_{t_{1u}}(R)$ ,  $D_d(R)$ , and the difference]. It is clear that the excess electrons extend outside the  $C_{60}$  radius (at 3.55 Å) and are much more delocalized than the  $t_{1u}$ -derived states. The spilling out of the molecular states is an electrostatic effect, resulting mainly from the presence of positive charges in the interstitial region and also from electron-electron repulsion on the molecule due to the charge transfer. In spite of the different crystal structure, and thus of the distribution of the positive charges, the spherical distribution of the excess electrons (not only that of the  $t_{1u}$ -derived states) is the same for  $K_3C_{60}$  and  $K_6C_{60}$ , the curves differing only by a factor of 2.

It is of some interest for a possible modeling of these

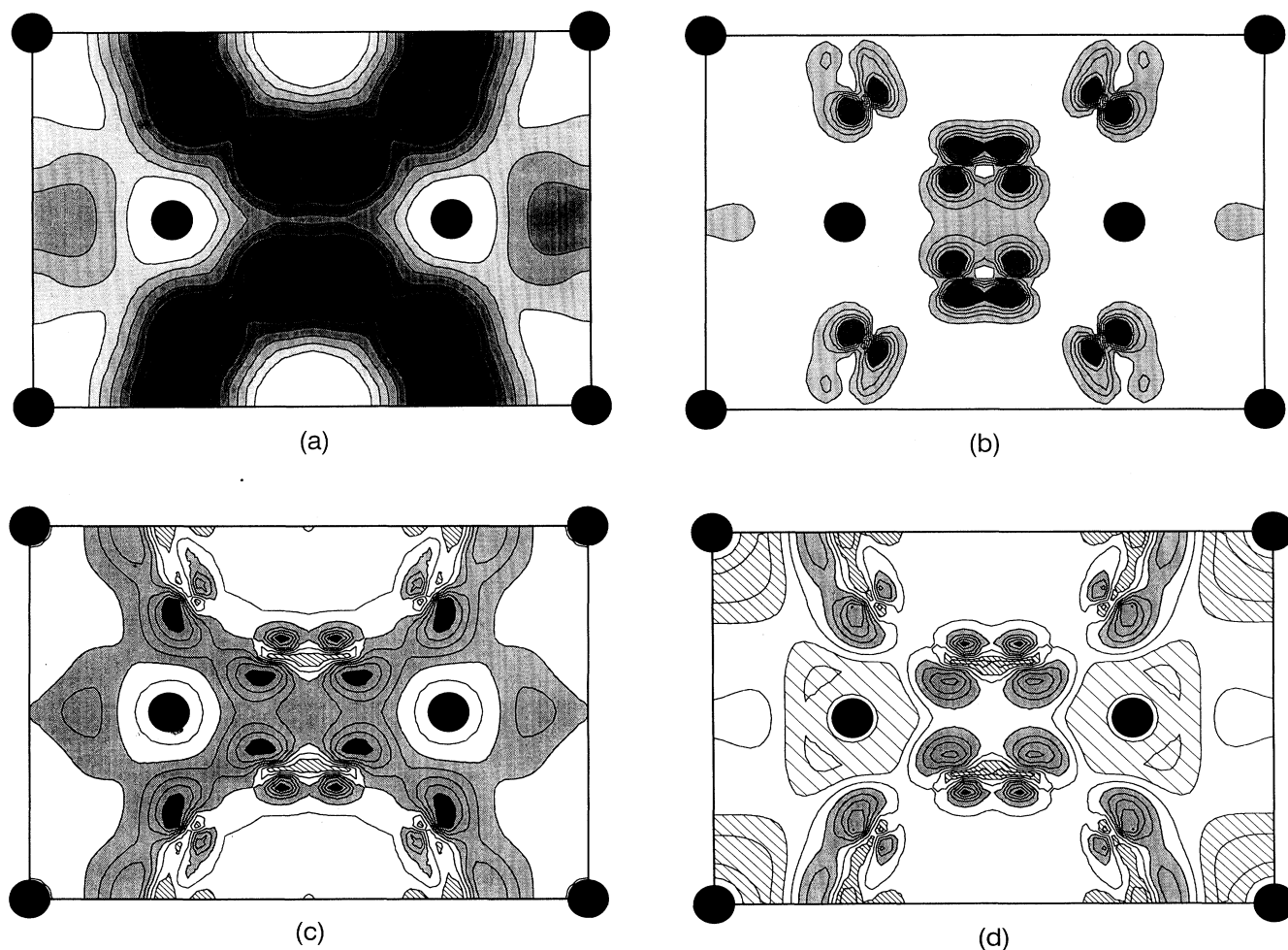


FIG. 4.  $K_3C_{60}$ , (110) plane. (a) Valence electron density  $\rho(r)$ ; (b) density of the  $t_{1u}$  derived states; (c) difference density  $\Delta_d(r)$ ; (d) transfer density  $\Delta_t(r)$ . In (a) contours scale logarithmically from 0.001 to 0.01  $e/(\text{a.u.})^3$ . In (b)–(d), contours vary linearly with 0.0005 spacing; white: interval from  $-0.0005$  to  $0.0005$ , hatched:  $< -0.0005$ .

systems to see to what extent the degree of charge transfer and the polarizability depend on the structural relaxation of the molecule. The answer comes from comparison with the same type of calculations performed by keeping the  $C_{60}$ 's in the molecular structure. The dependence is very weak so that Fig. 6, for instance, once obtained from consistent calculations with  $C_{60}$  kept in the molecular structure, is exactly the same.

$\Delta_t(r)$  is the quantity that describes the charge transfer. The plots in Figs. 4(d) and 5(d) show that charge flows from the alkali metals to the surrounding molecules in both compounds. The same message is apparent in

Fig. 7, where we plot the integrated charge  $I_{t_{1u}}(R)$  and transfer charge  $D_t(R)$  on spheres centered at the K positions. This picture of strongly ionic compounds agrees with previous calculations.<sup>12,19,20</sup> In  $K_3C_{60}$ , Fig. 7(a) also shows that the environment of the  $K_O$  atom is electronically poorer than that of the  $K_T$  atom. The integrals on the WS-like cells (Table III) give the same result by attributing  $0.3e$  to  $K_T$  and  $0.2e$  to  $K_O$ . This could naively be interpreted as a sign of stronger ionization of the potassium on the octahedral site. However, as already mentioned above, all the valence electron states have molecular character. Thus this finding does not

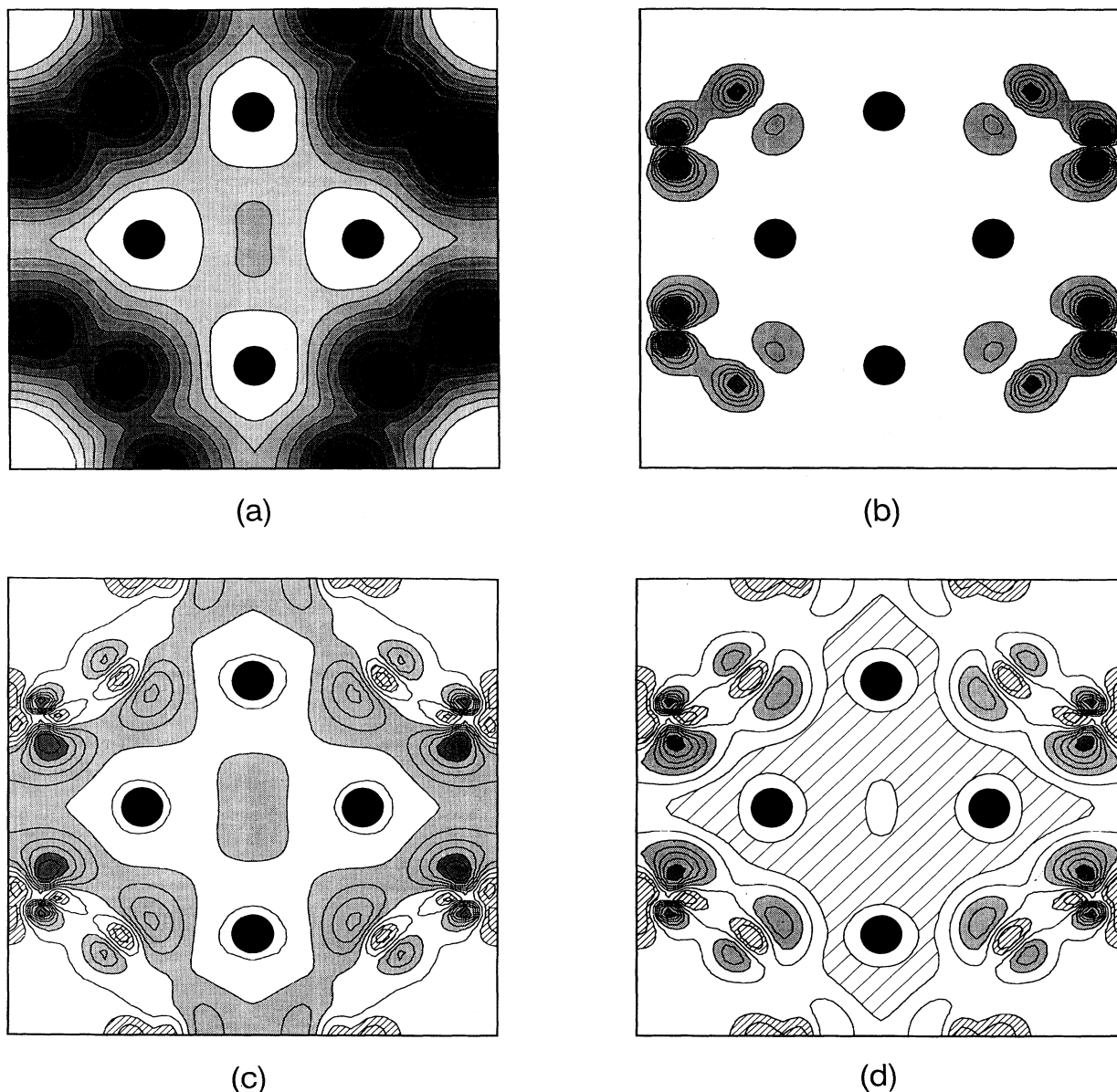


FIG. 5.  $K_6C_{60}$ , (100) plane. (a) Valence electron density  $\rho(r)$ ; (b) density of the  $t_{1u}$ -derived states; (c) difference density  $\Delta_d(r)$ ; (d) transfer density  $\Delta_t(r)$ . In (a) contours scale logarithmically from 0.001 to 0.01  $e/(\text{a.u.})^3$ . In (b)–(d), contours vary linearly with 0.001 spacing; white: interval from  $-0.001$  to  $0.001$ ; hatched:  $< -0.001$ .

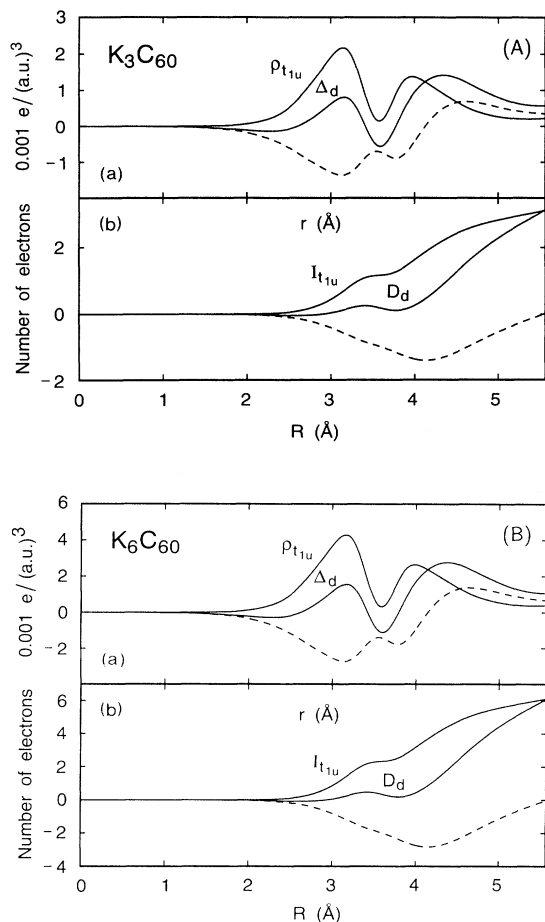


FIG. 6.  $K_3C_{60}$  (A) and  $K_6C_{60}$  (B). (a) Spherical average of the difference density  $\delta_d(r)$ , of the density of the  $t_{1u}$ -derived states, and their difference (dashed line). (b) Integrals as a function of the sphere radius. 0 is the center of  $C_{60}$ .

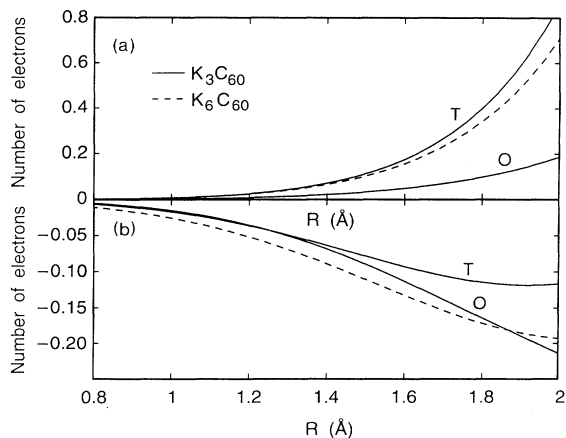


FIG. 7.  $K_3C_{60}$  (solid lines) and  $K_6C_{60}$  (dashed line). Spherical integrals of the valence electron density and of the transfer density as a function of the radius of the sphere centered at the K positions ( $R = 0$ ).

TABLE III. Valence charges  $Q_v$  calculated for different models (see text). In (a) charges are ascribed only to the C's; in (b) also to the K's.

Compound	C <sub>1</sub>	C <sub>2</sub>	C <sub>3</sub>	K <sub>T</sub>	K <sub>O</sub>
$K_3C_{60}$ (a)	4.060	4.055	4.040		
$K_3C_{60}$ (b)	4.043	4.042	4.028	0.301	0.204
Compound	C <sub>1</sub>	C <sub>2</sub>	C <sub>3</sub>	K	
$K_6C_{60}$ (a)	4.135	4.094	4.089		
$K_6C_{60}$ (b)	4.087	4.060	4.065	0.323	

reflect hybridization with K electron states, but purely geometrical facts,  $K_T$  being closer to the carbon shell than  $K_O$  is (see Table II) and having a larger number of carbons in the coordination shell (24 instead of 12). Moreover, consistent with the observation in Fig. 6(A), the charge diffused in the interstitial region is due to the spilling out of the orbitals lower than the  $t_{1u}$ -derived ones. The density associated with the latter is well confined to the individual molecules. Figure 8 shows  $\rho_{t_{1u}}$  around the K's in  $K_3C_{60}$ . It is vanishingly small over a radius of  $\approx 2$  Å in both cases, a value large compared to the core size of  $\approx 0.9$  Å. The WS integrals of  $\rho_{t_{1u}}$ ,  $Q_c$ , show that only  $0.03e$  (out of  $3e$ ) are in the interstitial regions around the K's. In  $K_6C_{60}$ , the value of  $Q_c$  is larger. Still, out of  $6e$ , only  $0.2e$  are in the interstitial region.

The high degree of ionization of the K atoms in  $K_3C_{60}$  is experimentally well established. The evidence consists of the measured  $g$  value,<sup>52</sup> which is typical of radical anions of  $C_{60}$ , as well as of the small diamagnetic shift of the  $^{39}K$  NMR resonance (measured with respect to KF).<sup>8</sup> We also note that, consistent with our findings, the  $^{39}K$  NMR spectrum<sup>8</sup> consists of two distinct resonance lines, with the larger shift corresponding to the minority ions, i.e., to the  $K_O$ 's.

The crystal field splits the carbon positions into three nonequivalent sets. In  $K_6C_{60}$ , the close environment of the  $C_2$  and  $C_3$  atoms is similar but noticeably different

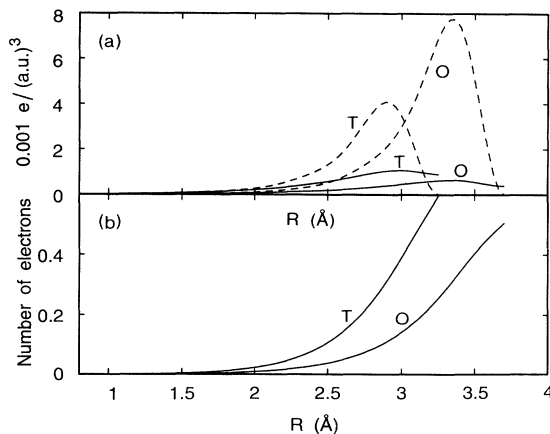


FIG. 8.  $K_3C_{60}$ . (a) Density of the  $t_{1u}$ -derived states [spherical average (solid line) and on the line joining K to the closest C (dotted line)] and (b) its spherical integral as a function of the sphere radius. 0 is the K position.

from that of  $C_1$ . In fact, the latter is much farther (by about 1 Å) from the other molecules and has three neighboring K's instead of two. In  $K_3C_{60}$ ,  $C_2$  and  $C_3$  have the same K environment (see Table II) at variance with  $C_1$ , but  $C_3$ 's correspond to the closest intermolecular distance. The distortion of the molecular structure due to the presence of the alkali-metal atoms in principle enhances the geometrical inequivalence. This is seen in the splittings of both hexagon-hexagon edges and hexagon-pentagon edges and of the radii, as seen in Table II and discussed above. These are, however, rather moderate, and especially so for  $K_3C_{60}$ .

The charge density integrals  $Q_v$  in Table III give us an idea of the extent to which the structural difference is reflected in the chemical inequivalence. We have performed the WS integrals in two different schemes: In one we have attributed the charge  $Q_v$  to all the atoms (a); in the other only to the fullerene (b). In the case of  $K_3C_{60}$ , the outcome is self-explanatory, especially the fact that the "inequivalence" signs are weak, independent of whether we include the K's. Also, in both schemes, the  $C_3$  atom turns out to be slightly electron poorer. In the case of  $K_6C_{60}$ , such inequivalence is more pronounced, with the  $C_1$  atom being the more electron-rich one.

The results in Table III are largely independent of whether we relax the structure of the  $C_{60}$  molecule. Also, they are roughly consistent with the Mulliken population analysis<sup>12,20</sup> derived from previous LDA calculations on  $K_6C_{60}$ , with fixed molecular structure. These calculations assigned excess charges of 0.12, 0.08, and 0.07 to the  $C_1$ ,  $C_2$ , and  $C_3$  atoms, respectively, and 0.17 to K. Discrepancies are an obvious consequence of the different definition used for these charges.

$^{13}C$  NMR experiments can in principle probe the magnetic inequivalence of the carbon atoms, which does not necessarily mirror their "chemical" inequivalence. Also, the interpretation of NMR data is far from being direct. In the case of  $K_6C_{60}$ ,  $^{13}C$  magic-angle spinning (MAS) NMR measurements at room temperature<sup>53,54</sup> clearly reveal three lines in the isotropic resonance, thus supporting the XRD image of an orientationally ordered phase. The shift with respect to  $C_{60}$  is paramagnetic and the explanation is not clear at all.<sup>54</sup> The smaller shift (at 153.1 ppm) corresponds to the minority  $C_1$  atoms, and the other two (unidentifiable) shifts are only very slightly split (155 ppm and 155.9 ppm). In a naive picture, this would be consistent with the presence of less valence charge around  $C_1$ . This, however, is clearly not valid, on the basis of the above discussion. The extension of the  $t_{1u}$ -derived orbitals occupied by the six extra electrons, instead, is such that  $C_1$  is appreciably poorer. This is reported in Table IV, and can also be seen in Fig. 9, where two three-dimensional isodensity surfaces are plotted.

In  $K_3C_{60}$ , the interpretation of the static NMR spectrum is even more complicated, because the metallic nature adds specific contributions of the conduction electrons (Knight shift), and because the rotation of the molecules can change the chemical environment of the C atoms with varying temperature in an uncontrolled manner. Earlier measurements on  $K_3C_{60}$  (Ref. 55) showed the existence of three different shifts, whose values and

TABLE IV. Charges  $Q_e$  associated with the  $t_{1u}$ -derived states and calculated for different models (see text). In (a) charges are ascribed only to the C's; in (b) also to the K's.

Compound	$C_1$	$C_2$	$C_3$	$K_T$	$K_O$
$K_3C_{60}$ (a)	0.052	0.050	0.049		
$K_3C_{60}$ (b)	0.051	0.050	0.048	0.010	0.012
fcc $C_{60,m}$	0.050	0.051	0.049		
Compound	$C_1$	$C_2$	$C_3$	K	
$K_6C_{60}$ (a)	0.086	0.104	0.103		
$K_6C_{60}$ (b)	0.082	0.101	0.100	0.035	
bcc $C_{60,m}$	0.088	0.103	0.103		

intensities were indeed temperature dependent, analogous to the behavior observed in  $Rb_3C_{60}$ .<sup>56</sup> More recent high-resolution data at low temperature<sup>54</sup> only detect one narrow line, whose anomalous shape, however, is interpreted as resulting from the contribution of different "frozen in" molecular orientations.

An inhomogeneous NMR spectral distribution also results from the nuclear relaxation rate  $T_1$  measured in the range 8–100 K.<sup>57</sup> The inhomogeneity of the conduction electron distribution at the molecular level, instead, has been proposed in Ref. 57 as one of the possible explanations.  $T_1$  has been analyzed in terms of three different rates pertaining to the three inequivalent C's, and a large difference between them has been obtained. Antropov *et al.*<sup>58</sup> have explicitly calculated  $T_1$  in the LDA approach, with the linear-muffin-tin-orbitals method, using as a model an ordered crystal structure like ours and an unrelaxed carbon molecule. They found that  $T_1$  is dominated by the spin-dipolar coupling, which in turn is essentially due to the  $p$  components of the  $t_{1u}$ -derived states, and that the contributions of the three carbon atoms were the same within 10%. In order to account for the apparently larger discrepancy, Holczer *et al.*<sup>57</sup> suggested the relaxation of the molecular structure as a possible addi-

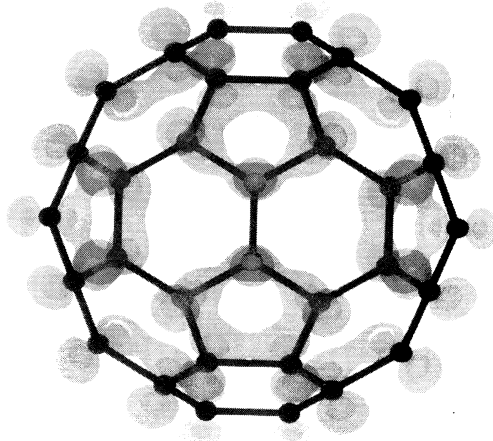


FIG. 9.  $K_6C_{60}$ . Constant density surfaces 0.005 (light) and 0.01 (dark)  $e/(a.u.)^3$  of the  $t_{1u}$ -derived states.

tional source of inequivalence for the three carbon atoms. However, as explained above, and as also confirmed by our calculations of the  $Q_c$  integrals, all the characteristics of the excess electrons that we calculate do not change on passing from the unrelaxed to the relaxed structure. Thus it seems improbable that molecular relaxation is sufficient to alter the conclusions drawn in Ref. 58. Other causes for such a discrepancy must be invoked. We note that, for instance, the model used for the crystal structure by Antropov *et al.*<sup>58</sup> and by us is oversimplified. A better model is one with two molecules per unit cell, accounting for their bidirectionality, where the site degeneracies are further split. Tight-binding calculations of the conduction band of  $C_{60}$  also show an increase of the overlap of the  $t_{1u}$ -derived states,<sup>23</sup> with respect to the unidirectional structure.

### C. Electron energy bands

The Kohn-Sham energy bands, although not representing the electronic excitation energies, generally constitute a sound starting point for the discussion of the main characteristic of the electronic structure of these compounds. LDA bands have been calculated many times (see, for instance, Refs. 12 and 19), and the extent to which they fail to give the measured band gaps and bandwidths has been discussed (see, e.g., Ref. 22). In the case of the  $C_{60}$  fullerite, the agreement with experiments has been obtained only at the *GW* level of theory.<sup>59</sup>  $K_3C_{60}$  is more complex. Electron-phonon coupling as well as electron-plasmon coupling effects must be taken into account to explain the photoemission data, for instance.<sup>26</sup> The purpose of our calculations was to identify the influence of the change of the molecular structure on the spectrum of the LDA bands, an effect hitherto ignored, and which we expect to be of the same order if introduced in more sophisticated calculations. Table V contains the values of a few energy gaps and bandwidths, calculated at various levels, as explained above. The decrease of the  $C_{60}$  gap between the highest occupied (HOMO) and lowest unoccupied (LUMO) molecular orbitals is an effect of the charge transfer and is mainly associated with the reduction of the bond alternation in the molecule. As expected, the effect of intercalation is larger in the saturated phase. However, from the comparison of  $K_6C_{60}$  with the  $C_{60}$  fcc fullerite it is clear that a major role is played by the difference in the crystal structure, as can be seen by comparing the two calculations for fcc  $C_{60,m}$  and bcc  $C_{60,m}$ .

## IV. CONCLUSIONS

We have presented the results of LDA calculations of  $K_6C_{60}$  and  $K_3C_{60}$ , in the conventional models for the crystal structure, aimed (i) to establish the characteristics of their chemical bonding, (ii) to determine the relaxation of the molecular structure and its driving mech-

TABLE V.  $K_3C_{60}$  and  $K_6C_{60}$ : some features of the LDA bands (in eV).  $E_g^{HL}$  is the HOMO-LUMO gap of  $C_{60}$ ,  $W_{k,k'} = E(k) - E(k')$  is the largest bandwidth calculated. “ $t_{1u}$ ” and “ $h_u$ ” are the band states derived from the LUMO and the HOMO of  $C_{60}$ , respectively.  $\Delta$  is the difference between the value calculated for the fulleride after relaxation and that of the molecule in the same lattice.

Compound	$E_g^{HL}(\Gamma)$	$E_g^{HL}(X)$	$W_{\Gamma,X}(\text{“}t_{1u}\text{”})$	$W_{X,\Gamma}(\text{“}h_u\text{”})$
fcc $C_{60,m}$	1.70	1.13	0.28	0.61
$K_3C_{60,m}$	1.72	1.12	0.27	0.68
$K_3C_{60}$	1.61	0.99	0.26	0.72
$\Delta$	-0.09	-0.14	-0.02	0.11
Compound	$E_g^{HL}(\Gamma)$	$E_g^{HL}(H)$	$W_{\Gamma,H}(\text{“}t_{1u}\text{”})$	$W_{H,\Gamma}(\text{“}h_u\text{”})$
bcc $C_{60,m}$	2.13	0.95	0.43	0.99
$K_6C_{60,m}$	2.17	0.66	0.50	1.13
$K_6C_{60}$	1.99	0.48	0.46	1.04
$\Delta$	-0.14	-0.47	0.03	0.05

anisms, as well as (iii) to identify its influence on several measurable electronic properties of the compounds.

In the case of  $K_6C_{60}$ , for which our study is more complete due to the absence of orientational disorder in the real compound, our results are more instructive. There, the effects of molecular relaxation on the features of the electron energy bands are also sizable. Ideally, one should compare structural and electronic properties with NMR spectra, which account for both. It is clear, however, that the correct interpretation of such data is rather complex and requires at least *ab initio* calculations of this type for the response of the system to an applied magnetic field, and in particular of quantities such as chemical shifts<sup>60</sup> and the hyperfine coupling tensor.<sup>58</sup> This is not possible with our present scheme. Examination of the picture of the electronic structure that our calculations provide, however, discourages naive interpretations of chemical shifts (based exclusively on charge transfer effects) for the saturated phase, and suggest “revisiting”  $^{13}C$  NMR data on  $K_3C_{60}$  with a more complex structural model in mind.<sup>11,35</sup>

While we have established the dominant “on-ball” effects of potassium intercalation, its influence on the intermolecular interactions is an important issue still waiting to be tackled with *ab initio* approaches. At the moment, the entire study of orientational disordering in  $C_{60}$  as well as in the  $x = 3$  phases relies on semiempirical models at best. Their validity, however, may be affected by the effects of electronic polarization, which the present calculations find to be rather important.

## ACKNOWLEDGMENTS

It is a pleasure to thank K. Holczer for several stimulating discussions. We also wish to thank F. Rachdi, J. E. Fischer, W. F. I. David, P. Bernier, and C. S. Yan-noni for useful comments and for communicating unpublished results. During the development of this work, we have also enjoyed discussions with F. Gygi, E. Tosatti, L. Pietronero, A. Curioni, and E. Fois.

- \* Present address: Max-Planck-Institut für Festkörperforschung, D-70569 Stuttgart, Germany.
- <sup>1</sup> R.C. Haddon, *Acc. Chem. Res.* **25**, 127 (1992).
  - <sup>2</sup> *Physics and Chemistry of Fullerene-Based Solids-II*, edited by J.E. Fischer, Y. Maruyama, D.E. Cox, and R.N. Shelton, special issue of *J. Phys. Chem. Solids* **54** (1993).
  - <sup>3</sup> *Physics and Chemistry of Fullerenes*, edited by K. Prasadides (Kluwer, Dordrecht, 1994).
  - <sup>4</sup> A.F. Hebard, M.J. Rosseinsky, R.C. Haddon, D.W. Murphy, S.H. Glarum, T.T.M. Palstra, A.P. Ramirez, and A.R. Kortan, *Nature (London)* **350**, 600 (1991).
  - <sup>5</sup> K. Holczer, O. Klein, G. Grüner, J.D. Thompson, F. Diederich, and R.L. Whetten, *Phys. Rev. Lett.* **67**, 271 (1991).
  - <sup>6</sup> K. Holczer, O. Klein, S.-M. Huang, R. B. Kaner, K.-J. Fu, R.L. Whetten, and F. Diederich, *Science* **252**, 1154 (1991).
  - <sup>7</sup> O. Zhou, J.E. Fischer, N. Coustel, S. Kycia, O. Zhu, A.R. McGhie, W.J. Romanow, Jr., J.P. McCauley, Jr., A.B. Smith, and D. Cox, *Nature (London)* **351**, 6326 (1991).
  - <sup>8</sup> K. Holczer and R.L. Whetten, *Carbon* **30**, 1261 (1992).
  - <sup>9</sup> J.E. Fischer, in *Physics and Chemistry of Fullerenes* (Ref. 3).
  - <sup>10</sup> T. Yildirim, S. Hong, A.B. Harris, and E.J. Mele, *Phys. Rev. B* **48**, 12 262 (1993).
  - <sup>11</sup> M.S. Deshpande, S.C. Erwin, S. Hong, and E.J. Mele, *Phys. Rev. Lett.* **71**, 2619 (1993).
  - <sup>12</sup> S.C. Erwin, in *Buckminsterfullerenes*, edited by W.E. Billups and M.A. Ciufolini (VCH Publishers, New York, 1993), p. 217; S.C. Erwin and W.E. Pickett, *Science* **254**, 842 (1991).
  - <sup>13</sup> R.F. Kiefl, T.L. Duty, J.W. Schneider, A. MacFarlane, K. Chow, J.W. Elzey, P. Mendels, G.D. Morris, J.H. Brewer, E.J. Ansaldo, C. Niedermayer, D.R. Noakes, C.E. Stronach, B. Hitti, and J.E. Fischer, *Phys. Rev. Lett.* **69**, 2005 (1992).
  - <sup>14</sup> A. Jánossi, O. Chauvet, S. Pekker, J.R. Cooper, and L. Forró, *Phys. Rev. Lett.* **71**, 1091 (1993).
  - <sup>15</sup> M.A. Schlüter, M. Lannoo, M. Needels, G.A. Baraff, and D. Tománek, *Phys. Rev. Lett.* **68**, 526 (1992).
  - <sup>16</sup> C.M. Varma, J. Zaanen, and K. Raghavachari, *Science* **254**, 989 (1991).
  - <sup>17</sup> S. Chakravarty and S.A. Kivelson, *Europhys. Lett.* **16**, 751 (1991).
  - <sup>18</sup> W. Andreoni, in *Properties of New Materials: Fullerenes*, edited by H. Kuzmany, J. Fink, M. Mehring, and S. Roth (Springer, Berlin, 1993), Vol. 117, p. 85.
  - <sup>19</sup> J.L. Martins and N. Trouiller, *Phys. Rev. B* **46**, 1766 (1992).
  - <sup>20</sup> S.C. Erwin and M.R. Pederson, *Phys. Rev. Lett.* **67**, 1610 (1991).
  - <sup>21</sup> P.J. Benning, J.L. Martins, J.H. Weaver, L.P.F. Chibante, and R.E. Smalley, *Science* **252**, 1417 (1991); J.H. Weaver and D.M. Poirier, *Solid State Properties of Fullerenes and Fullerene-based Materials*, edited by H. Ehrenreich and F. Spaepen, *Solid State Physics* Vol. 48 (Academic Press, New York, 1984), Chap. I.
  - <sup>22</sup> J. Fink, E. Sohmen, M. Merkel, A. Masaki, H. Romberg, M. Alexander, M. Knupfer, M.S. Golden, P. Adelman, and B. Renker, in *Fullerenes: Status and Perspectives*, edited by C. Taliani, C. Ruani, and R. Zamboni (World Scientific, Singapore, 1992), p. 161.
  - <sup>23</sup> S. Satpathy, V.P. Antropov, O.K. Andersen, O. Jepsen, O. Gunnarsson, and A.I. Liechtenstein, *Phys. Rev. B* **46**, 1773 (1992).
  - <sup>24</sup> M.P. Gelfand and J.P. Lu, *Phys. Rev. Lett.* **68**, 1050 (1992).
  - <sup>25</sup> R.P. Gupta and M. Gupta, *Phys. Rev. B* **47**, 11 635 (1993).
  - <sup>26</sup> V.P. Antropov, O. Gunnarsson, and A.I. Liechtenstein, *Phys. Rev. B* **48**, 7651 (1993).
  - <sup>27</sup> R. Car and M. Parrinello, *Phys. Rev. Lett.* **55**, 2471 (1985).
  - <sup>28</sup> P.W. Stephens, L. Mihaly, P.L. Lee, R.L. Whetten, S.-M. Huang, R. Kaner, F. Diederich, and K. Holczer, *Nature (London)* **351**, 632 (1991).
  - <sup>29</sup> W. Andreoni, D. Scharf, and P. Giannozzi, *Chem. Phys. Lett.* **173**, 449 (1990).
  - <sup>30</sup> S.G. Louie, S. Froyen, and M.L. Cohen, *Phys. Rev. B* **26**, 1738 (1982).
  - <sup>31</sup> I. Moullet, W. Andreoni, and P. Giannozzi, *J. Chem. Phys.* **90**, 7306 (1989).
  - <sup>32</sup> U. Röthlisberger and W. Andreoni, *J. Chem. Phys.* **94**, 8129 (1991).
  - <sup>33</sup> For a test of convergence, see Ref. 29, and A. Curioni, P. Giannozzi, J. Hutter, and W. Andreoni (unpublished). Calculations at 55 Ry leave the bond lengths unchanged.
  - <sup>34</sup> D.J. Chadi and M.L. Cohen, *Phys. Rev. B* **8**, 5747 (1973).
  - <sup>35</sup> P.W. Stephens, L. Mihaly, J.B. Wiley, S. Huang, R.B. Kaner, F. Diederich, R.L. Whetten, and K. Holczer, *Phys. Rev. B* **45**, 543 (1992).
  - <sup>36</sup> *International Tables for X-ray Crystallography*, edited by N.F.M. Henry and K. Lonsdale (The Kynoch Press, Birmingham, 1952), Vol. I, No. 202, pp. 311 and 314.
  - <sup>37</sup> D.W. Murphy, M.J. Rosseinsky, R.M. Fleming, R. Tycko, A.P. Ramirez, R.C. Haddon, T. Siegrist, G. Dabbagh, J.C. Tully, and R.E. Walstedt, *J. Phys. Chem. Solids* **53**, 1321 (1992).
  - <sup>38</sup> Y. Yoshinari, H. Alloul, G. Kriza, and K. Holczer, *Phys. Rev. Lett.* **71**, 2413 (1993).
  - <sup>39</sup> R. Tycko, G. Dabbagh, M.J. Rosseinsky, D.W. Murphy, A.P. Ramirez, and R.M. Fleming, *Phys. Rev. Lett.* **68**, 1912 (1992).
  - <sup>40</sup> R. McWeeny, *Coulson's Valence* (Oxford University Press, New York, 1979), p. 246.
  - <sup>41</sup> L. Pietronero and S. Strässler, *Phys. Rev. Lett.* **47**, 593 (1983).
  - <sup>42</sup> B.P. Feuston, W. Andreoni, M. Parrinello, and E. Clementi, *Phys. Rev. B* **44**, 4056 (1991).
  - <sup>43</sup> This is the geometry considered in all previous calculations. See Refs. 19, 20, and 12.
  - <sup>44</sup> We remark that in a previous calculation on  $K_6C_{60}$  (Ref. 49), using the  $\Gamma$  point of the irreducible Brillouin zone, we had obtained stronger effects, and in particular a larger elongation of the  $C_1-C_1$  distance (1.447 Å instead of 1.428 Å). Also, for the fcc fullerenes  $K_3C_{60}$  and  $Na_6C_{60}$  (Ref. 51), we found that the  $\Gamma$  restriction results in an overestimate of the variations of the bond lengths with respect to the undoped system.
  - <sup>45</sup> K.M. Allen, W.F.I. David, J.M. Fox, R.M. Ibberson, and M.J. Rosseinsky (private communication).
  - <sup>46</sup> K. Prassides, C. Christides, I.M. Thomas, J. Mizuki, K. Tanigaki, and T.W. Ebbesen, *Science* **263**, 950 (1994).
  - <sup>47</sup> J. Kohanoff, W. Andreoni, and M. Parrinello, *Chem. Phys. Lett.* **198**, 472 (1992).
  - <sup>48</sup> O. Zhu, D.E. Cox, P.W. Stephens, and J.E. Fischer (private communication).
  - <sup>49</sup> W. Andreoni, F. Gygi, and M. Parrinello, *Phys. Rev. Lett.* **68**, 823 (1992).
  - <sup>50</sup> N.W. Ashcroft and N.D. Mermin, *Solid State Physics* (Holt, Rinehart and Winston, New York, 1976), p. 73.

- <sup>51</sup> W. Andreoni, P. Giannozzi, and M. Parrinello, *Phys. Rev. Lett.* **72**, 848 (1994).
- <sup>52</sup> P.M. Allemand, A.S. Koch, F. Wudl, Y. Rubin, F.N. Diederich, M.M. Alvarez, S.J. Anz, and R.L. Whetten, *J. Am. Chem. Soc.* **113**, 2780 (1991).
- <sup>53</sup> F. Rachdi, J. Reichenbach, L. Firlej, P. Bernier, M. Ribet, R. Aznar, G. Zimmer, M. Helmle, and M. Mehring, *Solid State Commun.* **87**, 547 (1993).
- <sup>54</sup> J. Reichenbach, F. Rachdi, I. Luk'yanchuk, M. Ribet, G. Zimmer, and M. Mehring, *J. Chem. Phys.* (to be published).
- <sup>55</sup> C.S. Yannoni, D.S. Bethune, J.R. Salem, and K. Holczer (unpublished).
- <sup>56</sup> C.S. Yannoni, H.R. Wendt, R.L. Siemens, J.R. Salem, D. Nguyen, J. Lyerle, R.D. Johnson, M. Hoinkis, M.S. deVries, R.S. Crowder, C.A. Brown, D.S. Bethune, L. Taylor, P. Jedrzejewski, and H.C. Dorn, *Synth. Met.* **59**, 279 (1993).
- <sup>57</sup> K. Holczer, O. Klein, H. Alloul, Y. Yoshinari, F. Hippert, S.-M. Huang, R.B. Kaner, and R.L. Whetten, *Europhys. Lett.* **23**, 63 (1993).
- <sup>58</sup> V.P. Antropov, I.I. Mazin, O.K. Andersen, A.I. Liechtenstein, and O. Jepsen, *Phys. Rev. B* **47**, 12 373 (1993).
- <sup>59</sup> E.L. Shirley and S.G. Louie, *Phys. Rev. Lett.* **71**, 133 (1993).
- <sup>60</sup> J. Cioslowski (unpublished).

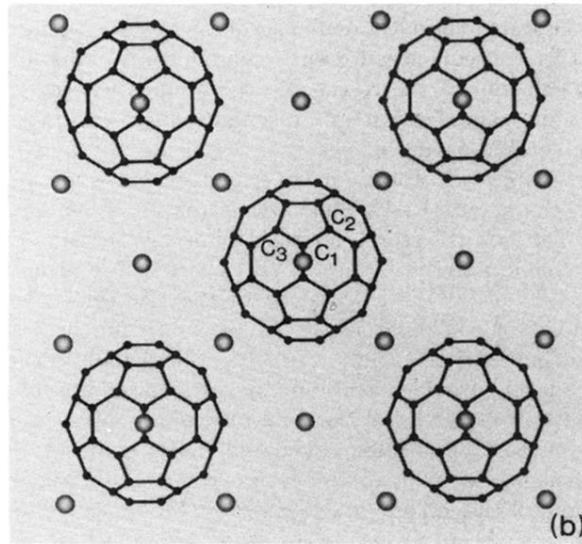
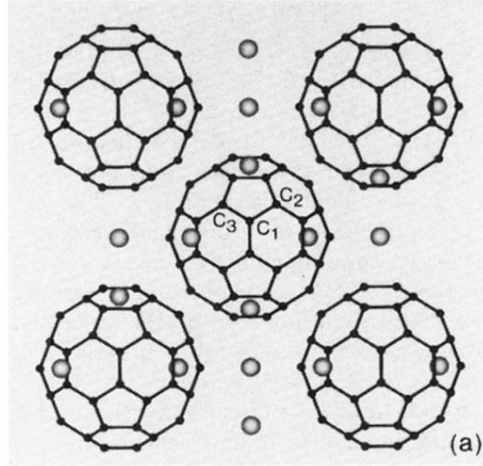


FIG. 1. Structure of the ordered configurations considered in the present work. (a) bcc  $K_6C_{60}$  (111) plane, and (b) fcc  $K_3C_{60}$  (100) plane.  $C_1$ ,  $C_2$ , and  $C_3$  denote the three inequivalent atoms.

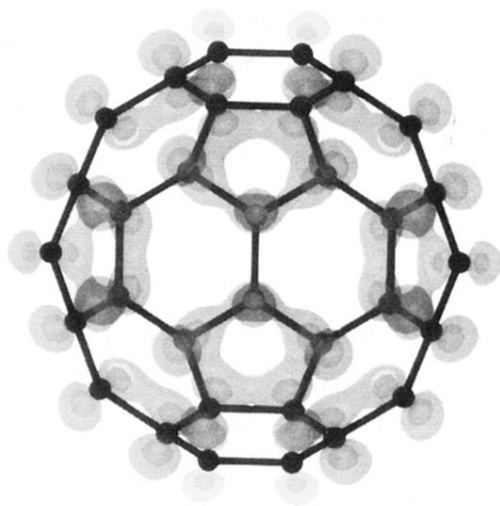


FIG. 9.  $K_6C_{60}$ . Constant density surfaces 0.005 (light) and 0.01 (dark)  $e/(\text{a.u.})^3$  of the  $t_{1u}$ -derived states.